Microbiology Spectrum
American Society for Microbiology Press

The Remarkable Biomechanical Properties of the Type 1 Chaperone-Usher Pilus: A Structural and Molecular Perspective

MANUELA K. HOSPENTHAL[1,2] and GABRIEL WAKSMAN[1]

[1]Institute of Structural and Molecular Biology, University College London and Birkbeck, London WC1E 7HX, United Kingdom; [2]Institute of Molecular Biology and Biophysics, ETH Zürich, 8093 Zürich, Switzerland

ABSTRACT Chaperone-usher (CU) pili are long, supramolecular protein fibers tethered to the surface of numerous bacterial pathogens. These virulence factors function primarily in bacterial adhesion to host tissues, but they also mediate biofilm formation. Type 1 and P pili of uropathogenic *Escherichia coli* (UPEC) are the two best-studied CU pilus examples, and here we primarily focus on the former. UPEC can be transmitted to the urinary tract by fecal shedding. It can then ascend up the urinary tract and cause disease by invading and colonizing host tissues of the bladder, causing cystitis, and the kidneys, causing pyelonephritis. FimH is the subunit displayed at the tip of type 1 pili and mediates adhesion to mannosylated host cells via a unique catch-bond mechanism. In response to shear forces caused by urine flow, FimH can transition from a low-affinity to high-affinity binding mode. This clever allosteric mechanism allows UPEC cells to remain tightly attached during periods of urine flow, while loosening their grip to allow dissemination through the urinary tract during urine stasis. Moreover, the bulk of a CU pilus is made up of the rod, which can reversibly uncoil in response to urine flow to evenly spread the tensile forces over the entire pilus length. We here explore the novel structural and mechanistic findings relating to the type 1 pilus FimH catch-bond and rod uncoiling and explain how they function together to enable successful attachment, spread, and persistence in the hostile urinary tract.

INTRODUCTION

Chaperone-usher (CU) pili are virulence factors displayed on a wide variety of Gram-negative bacterial pathogens (1), mediating bacterial attachment and biofilm formation (2). The two best-studied examples of CU pili are the type 1 and P pili of uropathogenic *Escherichia coli* (UPEC), which is the most important causative agent of urinary tract infections (3). We here summarize the steps of CU pilus biogenesis and highlight the most recent structural advances relating to type 1 pili that allow UPEC to thrive in the urinary tract.

BIOGENESIS OF CHAPERONE-USHER PILI

The individual building blocks required for type 1 and P pilus assembly are known as pilins (pilus subunits) and

Received: 30 August 2018, **Accepted:** 12 November 2018, **Published:** 25 January 2019

Editors: Maria Sandkvist, Department of Microbiology and Immunology, University of Michigan, Ann Arbor, Michigan; Eric Cascales, CNRS Aix-Marseille Université, Mediterranean Institute of Microbiology, Marseille, France; Peter J. Christie, Department of Microbiology and Molecular Genetics, McGovern Medical School, Houston, Texas

Citation: Hospenthal MK, Waksman G. 2019. The remarkable biomechanical properties of the type 1 chaperone-usher pilus: a structural and molecular perspective. *Microbiol Spectrum* 7(1): PSIB-0010-2018. doi:10.1128/microbiolspec.PSIB-0010-2018.

Correspondence: Manuela K. Hospenthal, manuela.hospenthal@mol.biol.ethz.ch; Gabriel Waksman, g.waksman@mail.cryst.bbk.ac.uk

are encoded by the *fim* and *pap* operons, respectively (4). The majority of fully assembled CU pili adopt a composite architecture consisting of a thin tip fibrillum, attached to a long superhelical rod emanating from the outer membrane (Fig. 1a). The adhesin (FimH for type 1 pili; PapG for P pili) is located at the distal end of the tip fibrillum and is composed of an N-terminal lectin domain, which is responsible for binding to specific host ligands, and a C-terminal pilin domain, which connects the adhesin to the remainder of the pilus (5, 6). The complete tip fibrillum is composed of further pilus subunits, namely, FimG and FimF in the case of type 1 pili or PapF, PapE, and PapK for P pili (Fig. 1a). The tip fibrillum of P pili is longer, as it contains 5 to 10 copies of PapE, while all other subunits are present as a single copy (7, 8). The largest section of CU pili, the rod, is composed of thousands of copies of a single pilin (FimA for type 1 pili; PapA for P pili) (2, 9, 10). All CU pilins are composed of C-terminally truncated and thus incomplete immunoglobulin (Ig)-like folds, lacking the 7th β-strand (Fig. 1b). Due to the missing strand, the pilins are unstable on their own and contain a long hydrophobic groove on their surface, composed of the so-called P1 to P5 hydrophobic pockets (6, 11). The pilins are stabilized by interacting with a dedicated chaperone (FimC for type 1 pili; PapD for P pili) through a process known as donor strand complementation (Fig. 1b). Here, the P1 to P4 pockets of the hydrophobic groove are complemented by residues of one of the chaperone's own β-strands, thereby completing the pilin's Ig-like fold, while the P5 pocket remains empty (6, 11–13). The chaperone-subunit complexes are then shuttled to the outer membrane-embedded usher (FimD for type 1 pili; PapC for P pili), where the pilus subunits are assembled into pili. During pilus assembly, pilins undergo a transition from a chaperone-stabilized binary complex to a stable polymer where the hydrophobic groove becomes complemented by a β-strand formed by the N-terminal extension (Nte) of the next subunit in assembly (14–16). This is termed donor strand exchange (DSE) (Fig. 1b).

The usher contains several distinct domains: the 24-stranded β-barrel pore, the N-terminal domain (NTD), two C-terminal domains (CTD1 and CTD2), and the plug (17, 18) (Fig. 1c). The steps of pilus biogenesis have been visualized by a series of structures and modeled states of the translocating usher of both the type 1 and P pilus systems (depicted in Fig. 1c). CU pili are assembled in a top-down manner starting with the adhesin, which primes the usher for pilus biogenesis when it is recruited to the periplasmic NTD (19–25). Next, the chaperone-adhesin complex is transferred to the higher-affinity CTDs, the plug is displaced from the usher pore into the periplasm, and the adhesin's lectin domain is translocated into the β-barrel channel (26, 27). This allows further chaperone-subunit complexes to be recruited to the NTD, bringing the Nte of the incoming subunit into close proximity with the hydrophobic groove of the preceding subunit (26). In a zip-in–zip-out mechanism, the P5 residue of the Nte first engages the previously empty P5 pocket before displacing the chaperone's donor strand entirely by sequentially invading the groove's P4, P3, P2, and P1 pockets (28, 29). The chaperone is recycled and further chaperone-subunit complexes continue to be incorporated into the growing pilus. The stochastic incorporation of PapH, the termination subunit of P pili, halts pilus biogenesis, as this subunit lacks the P5 pocket, making it unable to undergo DSE (30). FimI also displays a closed P5 pocket once bound to the NTD of the usher and is likely the termination subunit of type 1 pili (31). For a more detailed description of pilus biogenesis, please refer to recent reviews on this topic (2, 8, 32).

Two recent structures are beginning to shed light onto the handover mechanism of chaperone-subunit complexes from the NTD to the CTDs. First, a crystal structure of the "pre-activated" PapC usher, in complex with the chaperone-adhesin complex (PapDG), was determined (33) (Fig. 1d). In this structure, the PapDG complex has been recruited to the NTD but has not yet been fully transferred to the CTDs, while the plug still occupies the usher's β-barrel pore. Interestingly, CTD2 has moved across to engage PapDG bound to the NTD, by forming contacts with both PapD and the NTD. Thus, this state potentially represents the moment prior to chaperone-adhesin handover from the NTD to the CTDs in the preactivated usher. The precise temporal order of plug displacement, transfer to the CTDs, and recruitment of the next chaperone-subunit complex remains to be determined. Second, a new conformation of the activated usher during chaperone-subunit handover was captured using cryo-electron microscopy (34) (Fig. 1e). This structure of the FimD usher in complex with the tip fibrillum (FimFGH) and the chaperone (FimC) shows the usher in the process of chaperone-subunit (FimCF) handover to the CTDs. During this transfer, the NTD remains bound to the chaperone-subunit complex as it swings across to engage CTD2. At this point, both the NTD and CTD2 are bound to the growing end of the pilus, which has been suggested to prevent the pilus fiber from diffusing away during pilus biogenesis. This recent structural information, for both the preactivated (PapCDG) and activated (FimDCFGH) ushers during

chaperone-subunit transfer, raises interesting questions. While both structures revealed a novel interaction between the NTD and CTD2, the relative positions of the usher's various domains and the chaperone-subunit complex are distinct. Whether this is due to the stage of pilus biogenesis each structure represents (preactivated versus activated) and/or whether differences between the type 1 and P pilus systems also play a role remains to be fully explored.

MAKING CONTACT: THE ROLE OF THE TYPE 1 PILUS ADHESIN

UPEC can cause disease by ascending up the urinary tract and colonizing host tissues in the bladder (cystitis) and the kidney (pyelonephritis) (3, 35). The urinary tract presents a unique challenge for UPEC organisms, as they periodically experience the shear forces resulting from urine flow, which is faster and more turbulent in the bladder and lower urinary tract than in the kidneys (36). The adhesins of type 1 and P pili differ with respect to their ligands and their modes of interaction. The FimH lectin domain interacts with mannosylated proteins expressed on the surface of bladder epithelial cells with a so-called "catch-bond" mechanism, whereas the weaker "slip-bond" interaction of the PapG lectin domain with galabiose-containing glycosphingolipids takes place primarily on the kidney epithelium (8, 37–39). UPEC's ability to travel up the urinary tract is, in part, thought to involve an increase in P pilus expression and a concomitant downregulation of type 1 pilus expression (40). We here focus on recent advances in our understanding of the FimH-mannose catch-bond interaction.

The mannose binding site is located at the tip of FimH's lectin domain (Fig. 2a) and consists of a negatively charged pocket surrounded by a hydrophobic ridge (6, 41). In the ligand-bound state, the loops surrounding the binding site tighten around the ligand, with the most substantial rearrangement occurring in the clamp loop (residues 8 to 16) (42, 43) (Fig. 2b). Due to FimH's catch-bond mechanism, the affinity of its interaction with mannose increases when the bacterium experiences tensile mechanical force, as demonstrated in flow chamber (44, 45) and atomic force microscopy (46, 47) experiments. This allosteric mechanism depends on the relative orientation of FimH's lectin and pilin domains, which are connected by a linker (44) (Fig. 2a). FimH binds mannose with moderate affinity when the two domains are closely associated with each other and switches to a high-affinity binding mode when external forces (e.g., urine flow) separate the two domains. In a recent study, the binding kinetics of the FimH-mannose interaction were measured for donor strand-complemented full-length FimH (low-affinity state) and for the isolated lectin domain (a proxy for the high-affinity domain-separated state) (43). These measurements showed that in different *Escherichia coli* strains the low-affinity (domain-associated) state of FimH exhibits a dissociation constant in the micromolar range, whereas isolated lectin domains (high-affinity state) bound their ligands with ~3,300-fold-higher affinity in the low nanomolar range. This increase in affinity is due to a combination of a 30-fold-lower on-rate and >100,000-fold-lower off-rate (43).

The domain-separated high-affinity state is characterized by a rearrangement of the lectin domain's swing loop (residues 27 to 33), insertion loop (residues 112 to 118), and linker loop (residues 154 to 160), which form the interface with the pilin domain (42) (Fig. 2c). This conformational state has been observed in crystal structures of the isolated ligand-bound lectin domain (43, 48–53), FimH prior to DSE as observed in the FimCH (6, 41) and FimDCH complexes (26) (FimC keeps FimH in its domain-separated state), ligand-bound FimH complemented by a non-cognate donor strand peptide of FimF (43), and a FimH variant containing residues (A27V/V163A) that have been positively selected for pathogenicity among UPEC strains (54, 55). Structures of wild-type full-length FimH after DSE, either in the context of the remainder of the tip fibrillum (FimCFGH [42] and FimDCFGH [34, 56]) or complemented by a FimG Nte peptide (43, 54), adopt the low-affinity domain-associated conformation.

Early crystal structures capturing both high- and low-affinity states led to the proposition of an allosteric mechanism where domain separation induced by external forces caused a structural rearrangement of the lectin domain loops at the domain interface (Fig. 2c). These changes would, in turn, cause the β-sandwich lectin domain to adopt a less twisted and more elongated conformation, releasing the autoinhibitory effect of the pilin domain and resulting in the ligand binding loops tightening around the ligand (42) (Fig. 2b). Additional crystal structures, together with small-angle X-ray scattering (SAXS) and ion mobility-mass spectrometry (IMMS) experiments supported by molecular dynamics (MD), have further expanded the catch-bond mechanism. MD simulations showed that the relative conformational flexibility of the lectin and pilin domains is greater in the domain-separated state and that the overall conformation of the domain-associated state is fairly constrained (43, 54). Furthermore, the mode of ligand binding

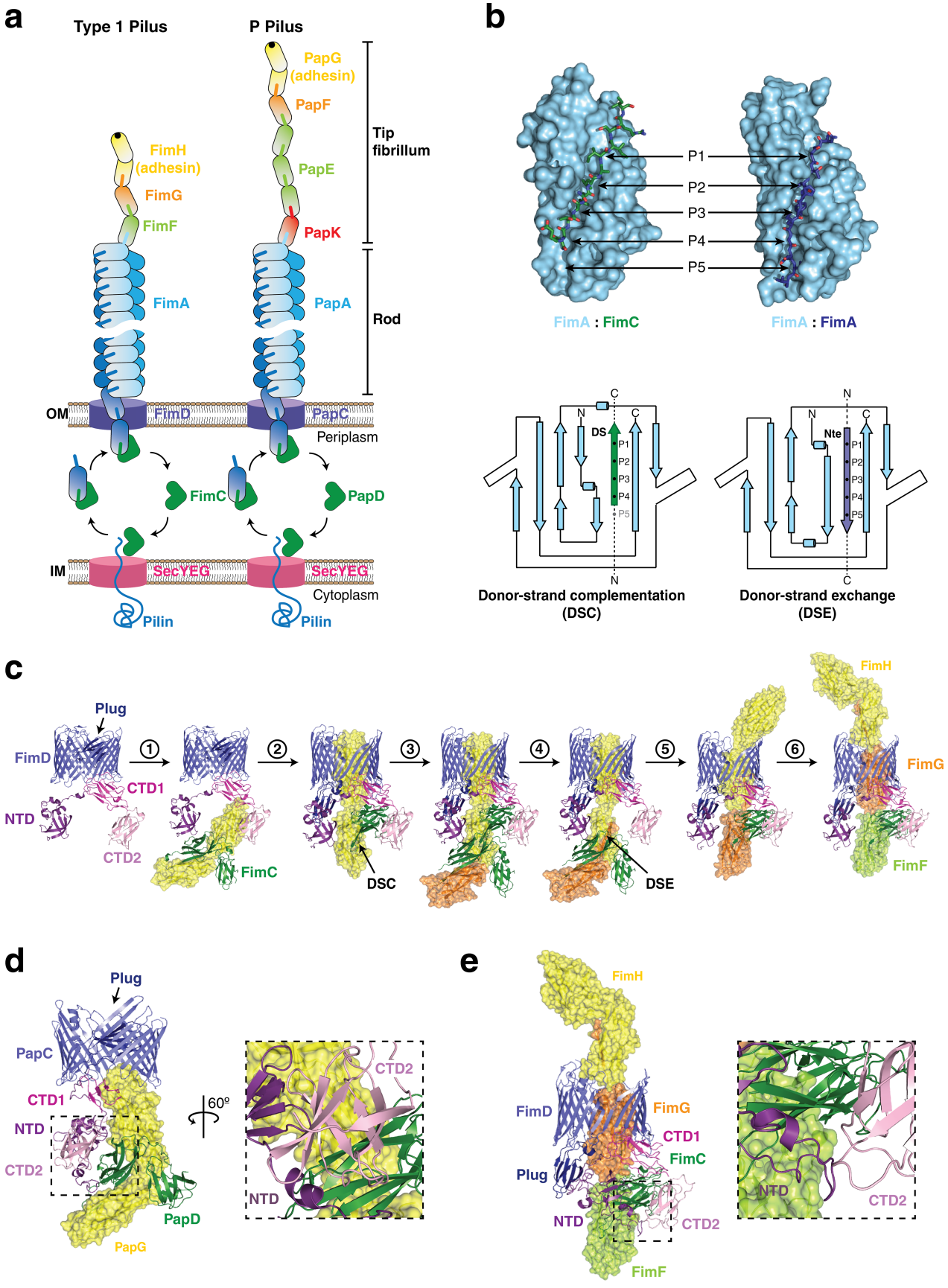

seemed to depend on the conformational state of FimH: in the domain-separated (high-affinity) state, the ligand bound tightly in a defined orientation (shown in Fig. 2b), whereas in the domain-associated (low-affinity) state, the ligand sampled several orientations (54). These simulations were in line with previous experiments that showed a high degree of conformational dynamics of the tyrosine gate (composed of two parallel tyrosines, Y48 and Y137) of the FimH binding pocket in the presence of mannosides (51, 57). On the other hand, crystal structures of both the high- and low-affinity states show the ligand bound in the same conformation, and the crystallographic B factors (temperature factor) of the bound ligand in these structures suggested that there is no difference in ligand binding mode (43). Furthermore, MD simulations suggested a high-energy barrier between the domain-associated and domain-separated states (43, 54), in agreement with ligand binding not leading to interface loop rearrangements and domain separation in crystal structures of donor strand-complemented full-length FimH (43). Nevertheless, insights from SAXS and IMMS experiments suggest that ligand binding may indeed start to shift the conformational equilibrium that exists in solution towards the domain-separated state (54).

This extraordinary catch-bond mechanism ensures that in the absence of urine flow, UPEC can overcome the strength of host cell binding to efficiently disseminate through the urinary tract using flagellar motility, while avoiding being flushed out during periods of urine flow (43, 45, 58, 59). In addition, the initial low-affinity interaction may prevent bacteria from engaging soluble mannose receptors, such as those on the Tamm-Horsfall protein, under low-shear conditions, which would constitute a nonproductive binding event (60).

CLINGING ON: THE IMPORTANCE OF THE PILUS ROD

The FimH catch-bond mechanism is not the only feature of type 1 pili that allows UPEC to biomechanically withstand the shear forces in the urinary tract. The rod, the largest CU pilus section, adopts a superhelical quaternary structure composed of 3 to 4 subunits (FimA for type 1 pili; PapA for P pili) per helical turn, with the most

FIGURE 1 Architecture and assembly of chaperone-usher pili. **(a)** Type 1 (left) and P pili (right) are the two archetypal CU pili of UPEC. Pilins are transported through the inner membrane (IM) via the SecYEG machinery. Once in the periplasm, a dedicated chaperone (FimC for type 1 pili; PapD for P pili) helps to fold, stabilize, and transport individual pilins to the outer membrane (OM), where they are assembled into pili by the usher (FimD for type 1 pili; PapC for P pili). The largest section of CU pili is the rod, which is composed of thousands of copies of a single subunit (FimA for type 1 pili; PapA for P pili) arranged into a right-handed superhelical quaternary structure. On top of the rod, located at the pilus' distal end, is a thin and flexible tip fibrillum. The most important tip fibrillum subunit is the adhesin (FimH for type 1 pili; PapG for P pili), which is responsible for the interaction of CU pili with host cell receptors. The remainder of the tip fibrillum is formed by FimG and FimF for type 1 pili and PapF, PapE, and PapK for P pili. **(b)** Pilins are unstable on their own because they consist of C-terminally truncated incomplete Ig-like folds lacking the 7th β-strand. This creates a large hydrophobic groove on the subunit's surface. After their transport into the periplasm, the chaperone inserts its G1 β-strand into the hydrophobic groove, thereby completing and stabilizing its fold. This is known as donor strand complementation (DSC) (PDB code 4DWH [79]) (left side). The pilin's P1 to P4 pockets are occupied by the chaperone's P1 to P4 residues, while the P5 pocket remains empty. Once assembled into a pilus, the 10- to 20-residue-long N-terminal extension (Nte) of each subunit complements the preceding pilin's groove, stabilizing the structure and linking the subunits in the pilin polymer. This is referred to as donor strand exchange (DSE) (PDB code 5OH0 [10]) (right side). The Nte of FimA in the surface model on the right has been removed for clarity. A zip-in–zip-out mechanism is responsible for the transition from DSC to DSE, whereby the previously empty P5 pocket first becomes occupied by the incoming subunit's Nte, displacing the chaperone's complementing strand and subsequently allowing the Nte to fully occupy the pilin's P1 to P5 pockets. **(c)** In step 1, the chaperone-adhesin complex binds to the usher's NTD (PDB codes 3BWU [80], 1QUN [6], and 3OHN and 3RFZ [26]). In step 2, the plug relocates next to the periplasmically located NTD, while the chaperone-adhesin complex is transferred to the usher's CTDs, which interact with the adhesin's pilin domain. The adhesin's lectin domain begins to translocate through the usher pore (PDB code 3RFZ). In step 3, the next chaperone-pilin complex is recruited to the NTD and the Nte of this pilin is oriented towards the pilin domain of the adhesin (PDB codes 3RFZ and 3BWU). In step 4, the chaperone's donor strand is replaced by the Nte of the newly recruited pilin by the zip-in–zip-out mechanism. The displaced chaperone is recycled (PDB codes 3RFZ, 3BWU, and 4XOE [43]). In step 5, the chaperone-pilin complex is transferred to the CTDs and the adhesin continues to move up and out through the usher pore (PDB codes 3RFZ and 4J3O [56]). In step 6, the cycle is repeated and new pilins are incorporated into the growing pilus (PDB code 4J3O). The mechanism of translocation through the usher depicted is illustrated using both crystal and modeled structures of the CU pilus systems. **(d and e)** Two novel structures shed light on the chaperone-subunit handover mechanism from the NTD to the CTDs. Shown are the structures of PapCDG (PDB code 6CD2 [33]) in a preactivated state **(d)** and of FimDCFGH (PDB code 6E14 [34]) in an activated state **(e)**, trapping conformations that show novel interactions between the NTD and CTD2, during chaperone-subunit handover. Dashed boxes and zoomed-in views highlight the NTD to CTD2 interactions.

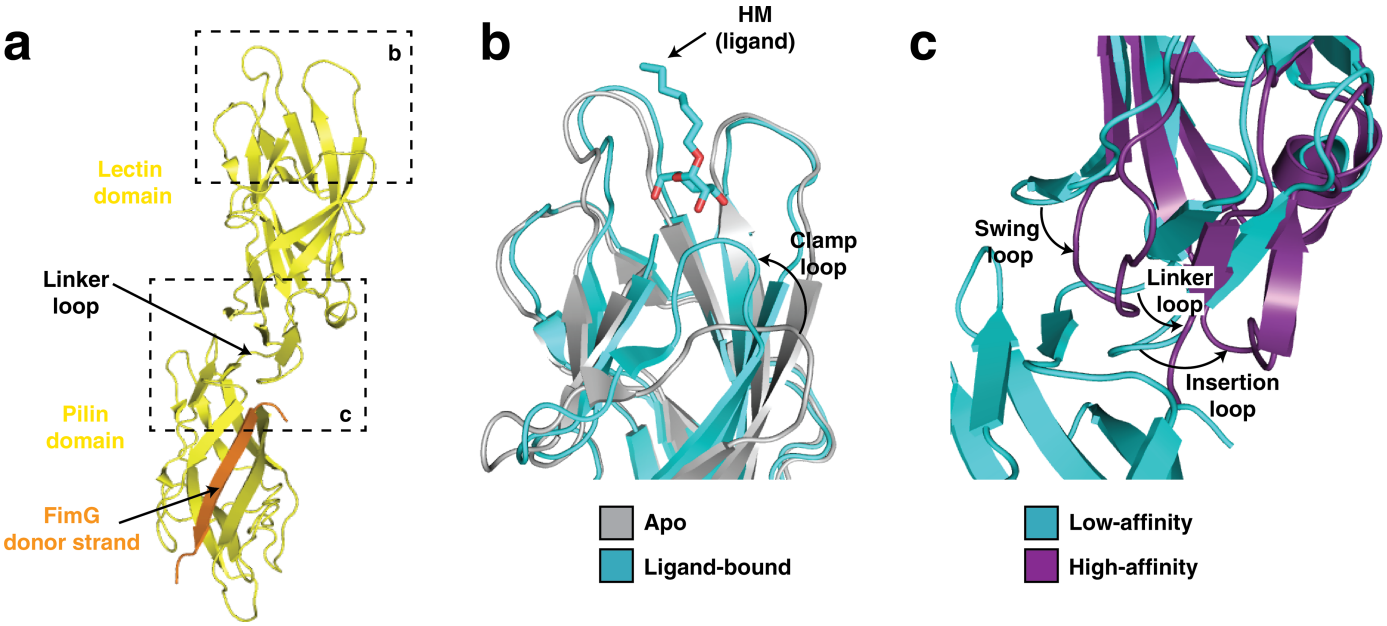

FIGURE 2 Structural rearrangements in FimH. **(a)** Ribbon diagram of full-length FimH (yellow), which is complemented by a donor strand peptide from FimG (orange) (PDB code 4XOE [43]). The lectin and pilin domains are labeled, and the dashed boxes highlight the ligand binding pocket (top) and the domain interface region (bottom) that are expanded in panels b and c. **(b)** Superposition of apo (gray) (PDB code 4XOD [43]) and ligand-bound (cyan) (PDB code 4XOE [43]) FimH, focusing on the ligand binding pocket. The ligand is *n*-heptyl α-D-mannoside (HM). An arrow indicates the structural rearrangement of the clamp loop. **(c)** Superposition of ligand-bound FimH (cyan) (PDB code 4XOE) and a ligand-bound construct of the FimH lectin domain only (purple) (PDB code 4XOC [43]), focusing on the lectin domain loops at the domain interface. The cyan structure is in a domain-associated (low-affinity) state, whereas the purple lectin domain-only structure represents the conformation of a domain-separated (high-affinity) state. Arrows indicate the rearrangements of the swing, linker, and insertion loops. The FimH pilin domain in all structures was stabilized by a FimG donor strand peptide.

important interface (stacking interface) occurring between every *n* and *n* + 3 subunits (61–63) (Fig. 3a and b). This remarkable structure is able to uncoil in response to shear forces, by sequentially breaking the stack-to-stack interactions, thereby dissipating the forces experienced by the adhesin and enabling UPEC to remain firmly attached (64, 65). The FimH catch-bond affinity switch and rod uncoiling mechanisms are functionally coupled, as the forces required for the two are similar (66, 67). In 2016, the first high-resolution cryo-electron microscopy structure of the P pilus revealed the molecular determinants that enable rod uncoiling (9). During urine flow, the DSE interactions that stabilize and link the pilins in the rod are extremely strong and will not break (68, 69) (Fig. 3c), whereas the largely polar interactions that mediate the subunit-subunit interactions of the rod's quaternary superhelical structure are much weaker and begin to break (9). This causes the rod to progressively uncoil, eventually adopting a head-to-tail configuration of pilins before recoiling once the external force has ceased. These biomechanical properties have been the subject of many atomic force microscopy and optical tweezer studies (36, 64–67, 70–77). Interestingly, such experiments showed that type 1 pilus rods require slightly higher forces to induce rod unwinding than do P pilus rods, prompting the suggestion that type 1 pili are better adapted to withstand the more turbulent flows of the lower urinary tract (36, 76). Several structures of the type 1 pilus rod have been determined (10, 77, 78) (Fig. 3), revealing a very similar overall architecture to the P pilus rod, except that the type 1 pilus rod lacks the so-called "staple" region (9) (Fig. 3c). It was suggested that the increased resistance against unwinding of type 1 pili could be explained, in part, by the larger stacking interface (10). The physiological relevance of these biomechanical properties was demonstrated when UPEC strains expressing type 1 pilus rods with weaker stack-to-stack interactions were significantly attenuated in

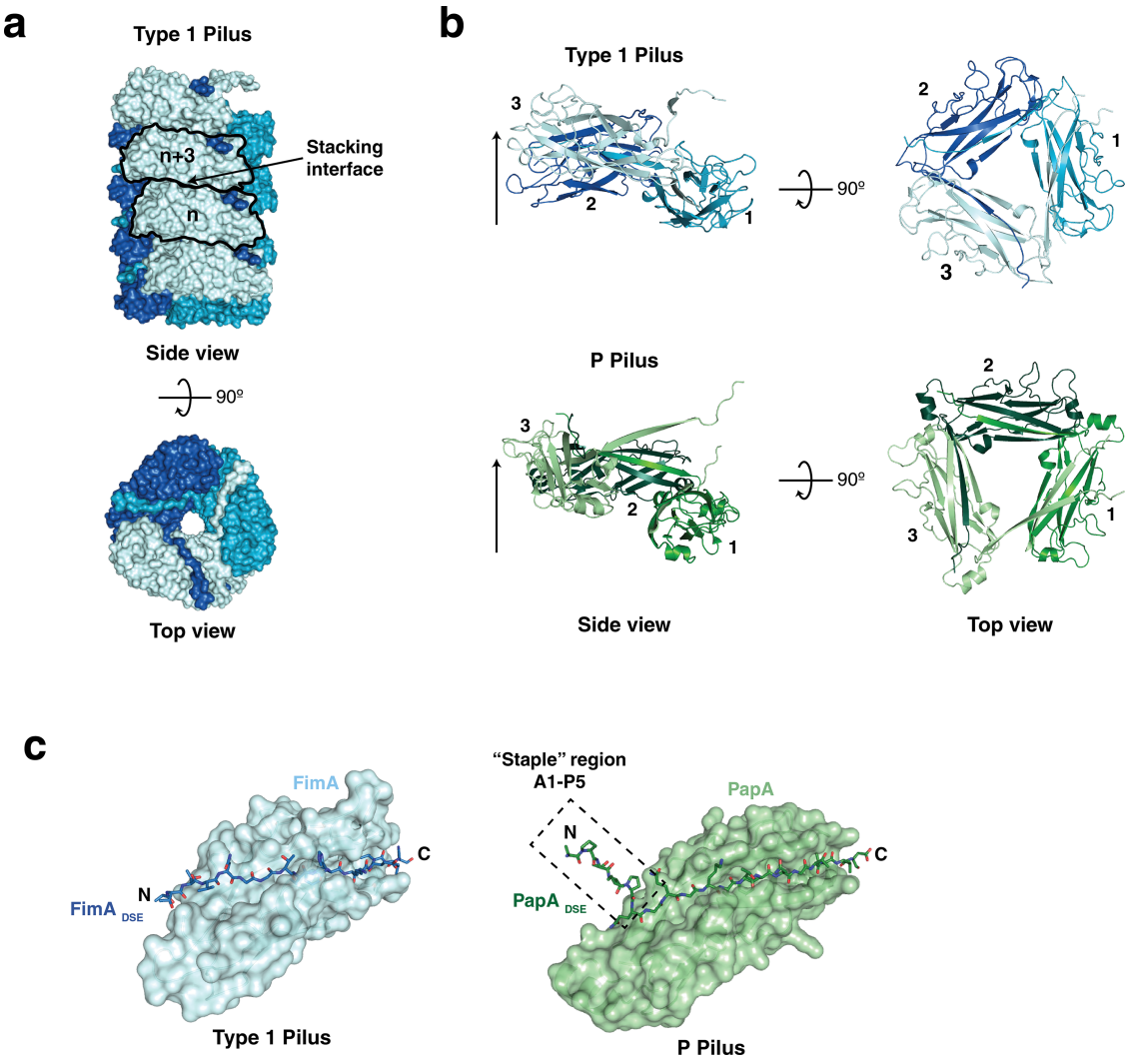

FIGURE 3 The structure of the rod. **(a)** Surface models showing the type 1 pilus rod structure (PDB code 5OH0 [10]) in a side view and a top view, which are 90° rotated with respect to each other. The Nte of the uppermost FimA molecule is removed in the top view for illustrative purposes. **(b)** Cartoon models showing three adjacent molecules or one "stack" of the type 1 pilus (blue) (PDB code 5OH0) and P pilus (green) (PDB code 5FLU [9]) rods. The left and right parts of this panel show one stack as a side view and a top view, respectively, rotated by 90°. Pilin subunits are arbitrarily numbered starting with the pilin at the bottom, which would be most proximal to the OM and last to be assembled, to show the nature of the right-handed superhelical structure. The arrow in the side view shows the upward trajectory of the subunits in the structure. **(c)** Surface representation of an individual FimA pilin subunit within the type 1 pilus rod (left, blue) (PDB code 5OH0) and a PapA pilin subunit within the P pilus rod (right, green) (PDB code 5FLU). The stick model shows the complementing donor strands, which originate from the Nte of the next subunit in assembly. The dashed box shows the staple region (residues 1 to 5) of the PapA Nte, a region not present in the type 1 pilus.

their ability to cause intestinal colonization and bladder infection in mice (77).

Interestingly, the stability of type 1 pili seems to depend on the route of their assembly. Type 1 pili assembled *in vivo*, by the CU machinery, are significantly more stable against dissociation and unfolding than pilus rods assembled from FimA alone *in vitro* (10). In fact, the unfolding rate constants differed by 3 to 4 orders of magnitude, raising the intriguing question of whether the usher, or indeed another factor, can guide and influence the assembly of an optimally stable structure *in vivo*. Future experiments will hopefully

resolve this question and reveal the molecular details responsible.

CONCLUSIONS

In this brief review, we have summarized aspects of CU pilus structure, with a special focus on type 1 pili. The FimH catch-bond mechanism and the spring-like properties of the rod are crucial biomechanical adaptations that allow UPEC to maintain a foothold in the hostile environment of the urinary tract. These two features are functionally coupled, and perturbation of either results in less virulent bacteria.

ACKNOWLEDGMENT

This work was funded by MRC grant 018434 to G.W.

REFERENCES

1. Thanassi DG, Saulino ET, Hultgren SJ. 1998. The chaperone/usher pathway: a major terminal branch of the general secretory pathway. *Curr Opin Microbiol* **1:**223–231. http://dx.doi.org/10.1016/S1369-5274(98)80015-5.

2. Hospenthal MK, Costa TRD, Waksman G. 2017. A comprehensive guide to pilus biogenesis in Gram-negative bacteria. *Nat Rev Microbiol* **15:**365–379. http://dx.doi.org/10.1038/nrmicro.2017.40.

3. Flores-Mireles AL, Walker JN, Caparon M, Hultgren SJ. 2015. Urinary tract infections: epidemiology, mechanisms of infection and treatment options. *Nat Rev Microbiol* **13:**269–284. http://dx.doi.org/10.1038/nrmicro3432.

4. Schwan WR. 2011. Regulation of *fim* genes in uropathogenic *Escherichia coli*. *World J Clin Infect Dis* **1:**17–25. http://dx.doi.org/10.5495/wjcid.v1.i1.17.

5. Dodson KW, Pinkner JS, Rose T, Magnusson G, Hultgren SJ, Waksman G. 2001. Structural basis of the interaction of the pyelonephritic *E. coli* adhesin to its human kidney receptor. *Cell* **105:**733–743. http://dx.doi.org/10.1016/S0092-8674(01)00388-9.

6. Choudhury D, Thompson A, Stojanoff V, Langermann S, Pinkner J, Hultgren SJ, Knight SD. 1999. X-ray structure of the FimC-FimH chaperone-adhesin complex from uropathogenic *Escherichia coli*. *Science* **285:**1061–1066. http://dx.doi.org/10.1126/science.285.5430.1061.

7. Kuehn MJ, Heuser J, Normark S, Hultgren SJ. 1992. P pili in uropathogenic *E. coli* are composite fibres with distinct fibrillar adhesive tips. *Nature* **356:**252–255. http://dx.doi.org/10.1038/356252a0.

8. Werneburg GT, Thanassi DG. 2018. Pili assembled by the chaperone/usher pathway in *Escherichia coli* and *Salmonella*. *Ecosal Plus* **8:**1–37. http://dx.doi.org/10.1128/ecosalplus.ESP-0007-2017.

9. Hospenthal MK, Redzej A, Dodson K, Ukleja M, Frenz B, Rodrigues C, Hultgren SJ, DiMaio F, Egelman EH, Waksman G. 2016. Structure of a chaperone-usher pilus reveals the molecular basis of rod uncoiling. *Cell* **164:**269–278. http://dx.doi.org/10.1016/j.cell.2015.11.049.

10. Hospenthal MK, Zyla D, Costa TRD, Redzej A, Giese C, Lillington J, Glockshuber R, Waksman G. 2017. The cryoelectron microscopy structure of the type 1 chaperone-usher pilus rod. *Structure* **25:**1829–1838.e4. http://dx.doi.org/10.1016/j.str.2017.10.004.

11. Sauer FG, Fütterer K, Pinkner JS, Dodson KW, Hultgren SJ, Waksman G. 1999. Structural basis of chaperone function and pilus biogenesis. *Science* **285:**1058–1061. http://dx.doi.org/10.1126/science.285.5430.1058.

12. Barnhart MM, Pinkner JS, Soto GE, Sauer FG, Langermann S, Waksman G, Frieden C, Hultgren SJ. 2000. PapD-like chaperones provide the missing information for folding of pilin proteins. *Proc Natl Acad Sci U S A* **97:**7709–7714. http://dx.doi.org/10.1073/pnas.130183897.

13. Vetsch M, Puorger C, Spirig T, Grauschopf U, Weber-Ban EU, Glockshuber R. 2004. Pilus chaperones represent a new type of protein-folding catalyst. *Nature* **431:**329–333. http://dx.doi.org/10.1038/nature02891.

14. Sauer FG, Pinkner JS, Waksman G, Hultgren SJ. 2002. Chaperone priming of pilus subunits facilitates a topological transition that drives fiber formation. *Cell* **111:**543–551. http://dx.doi.org/10.1016/S0092-8674(02)01050-4.

15. Zavialov AV, Berglund J, Pudney AF, Fooks LJ, Ibrahim TM, MacIntyre S, Knight SD. 2003. Structure and biogenesis of the capsular F1 antigen from *Yersinia pestis*: preserved folding energy drives fiber formation. *Cell* **113:**587–596. http://dx.doi.org/10.1016/S0092-8674(03)00351-9.

16. Nishiyama M, Ishikawa T, Rechsteiner H, Glockshuber R. 2008. Reconstitution of pilus assembly reveals a bacterial outer membrane catalyst. *Science* **320:**376–379. http://dx.doi.org/10.1126/science.1154994.

17. Remaut H, Tang C, Henderson NS, Pinkner JS, Wang T, Hultgren SJ, Thanassi DG, Waksman G, Li H. 2008. Fiber formation across the bacterial outer membrane by the chaperone/usher pathway. *Cell* **133:**640–652. http://dx.doi.org/10.1016/j.cell.2008.03.033.

18. Huang Y, Smith BS, Chen LX, Baxter RHG, Deisenhofer J. 2009. Insights into pilus assembly and secretion from the structure and functional characterization of usher PapC. *Proc Natl Acad Sci U S A* **106:**7403–7407. http://dx.doi.org/10.1073/pnas.0902789106.

19. So SS, Thanassi DG. 2006. Analysis of the requirements for pilus biogenesis at the outer membrane usher and the function of the usher C-terminus. *Mol Microbiol* **60:**364–375. http://dx.doi.org/10.1111/j.1365-2958.2006.05111.x.

20. Saulino ET, Thanassi DG, Pinkner JS, Hultgren SJ. 1998. Ramifications of kinetic partitioning on usher-mediated pilus biogenesis. *EMBO J* **17:**2177–2185. http://dx.doi.org/10.1093/emboj/17.8.2177.

21. Ng TW, Akman L, Osisami M, Thanassi DG. 2004. The usher N terminus is the initial targeting site for chaperone-subunit complexes and participates in subsequent pilus biogenesis events. *J Bacteriol* **186:**5321–5331. http://dx.doi.org/10.1128/JB.186.16.5321-5331.2004.

22. Nishiyama M, Vetsch M, Puorger C, Jelesarov I, Glockshuber R. 2003. Identification and characterization of the chaperone-subunit complex-binding domain from the type 1 pilus assembly platform FimD. *J Mol Biol* **330:**513–525. http://dx.doi.org/10.1016/S0022-2836(03)00591-6.

23. Henderson NS, Ng TW, Talukder I, Thanassi DG. 2011. Function of the usher N-terminus in catalysing pilus assembly. *Mol Microbiol* **79:**954–967. http://dx.doi.org/10.1111/j.1365-2958.2010.07505.x.

24. Nishiyama M, Horst R, Eidam O, Herrmann T, Ignatov O, Vetsch M, Bettendorff P, Jelesarov I, Grütter MG, Wüthrich K, Glockshuber R, Capitani G. 2005. Structural basis of chaperone-subunit complex recognition by the type 1 pilus assembly platform FimD. *EMBO J* **24:**2075–2086. http://dx.doi.org/10.1038/sj.emboj.7600693.

25. Munera D, Hultgren S, Fernández LÁ. 2007. Recognition of the N-terminal lectin domain of FimH adhesin by the usher FimD is required for type 1 pilus biogenesis. *Mol Microbiol* **64:**333–346. http://dx.doi.org/10.1111/j.1365-2958.2007.05657.x.

26. Phan G, Remaut H, Wang T, Allen WJ, Pirker KF, Lebedev A, Henderson NS, Geibel S, Volkan E, Yan J, Kunze MBA, Pinkner JS, Ford B, Kay CWM, Li H, Hultgren SJ, Thanassi DG, Waksman G. 2011. Crystal structure of the FimD usher bound to its cognate FimC-FimH substrate. *Nature* **474:**49–53. http://dx.doi.org/10.1038/nature10109.

27. Werneburg GT, Henderson NS, Portnoy EB, Sarowar S, Hultgren SJ, Li H, Thanassi DG. 2015. The pilus usher controls protein interactions via domain masking and is functional as an oligomer. *Nat Struct Mol Biol* **22:**540–546. http://dx.doi.org/10.1038/nsmb.3044.

28. Remaut H, Rose RJ, Hannan TJ, Hultgren SJ, Radford SE, Ashcroft AE, Waksman G. 2006. Donor-strand exchange in chaperone-assisted pilus assembly proceeds through a concerted beta strand displacement mechanism. *Mol Cell* **22:**831–842. http://dx.doi.org/10.1016/j.molcel.2006.05.033.

29. Rose RJ, Welsh TS, Waksman G, Ashcroft AE, Radford SE, Paci E. 2008. Donor-strand exchange in chaperone-assisted pilus assembly revealed in atomic detail by molecular dynamics. *J Mol Biol* **375:**908–919. http://dx.doi.org/10.1016/j.jmb.2007.10.077.

30. Verger D, Miller E, Remaut H, Waksman G, Hultgren S. 2006. Molecular mechanism of P pilus termination in uropathogenic *Escherichia coli*. *EMBO Rep* **7:**1228–1232. http://dx.doi.org/10.1038/sj.embor.7400833.

31. Bečárová Z. 2015. Mechanisms of FimI, the assembly termination subunit of the type 1 pili from uropathogenic *Escherichia coli*. PhD thesis. ETH Zürich, Zürich, Switzerland.

32. Waksman G. 2017. Structural and molecular biology of a protein-polymerizing nanomachine for pilus biogenesis. *J Mol Biol* **429:**2654–2666. http://dx.doi.org/10.1016/j.jmb.2017.05.016.

33. Omattage NS, Deng Z, Pinkner JS, Dodson KW, Almqvist F, Yuan P, Hultgren SJ. 2018. Structural basis for usher activation and intramolecular subunit transfer in P pilus biogenesis in *Escherichia coli*. *Nat Microbiol* **3:**1362–1368. http://dx.doi.org/10.1038/s41564-018-0255-y.

34. Du M, Yuan Z, Yu H, Henderson N, Sarowar S, Zhao G, Werneburg GT, Thanassi DG, Li H. 2018. Handover mechanism of the growing pilus by the bacterial outer-membrane usher FimD. *Nature* **562:**444–447. http://dx.doi.org/10.1038/s41586-018-0587-z.

35. Spaulding CN, Klein RD, Schreiber HL IV, Janetka JW, Hultgren SJ. 2018. Precision antimicrobial therapeutics: the path of least resistance? *NPJ Biofilms Microbiomes* **4:**4. http://dx.doi.org/10.1038/s41522-018-0048-3.

36. Andersson M, Uhlin BE, Fällman E. 2007. The biomechanical properties of *E. coli* pili for urinary tract attachment reflect the host environment. *Biophys J* **93:**3008–3014. http://dx.doi.org/10.1529/biophysj.107.110643.

37. Roberts JA, Marklund BI, Ilver D, Haslam D, Kaack MB, Baskin G, Louis M, Möllby R, Winberg J, Normark S. 1994. The Gal(alpha 1-4)Gal-specific tip adhesin of *Escherichia coli* P-fimbriae is needed for pyelonephritis to occur in the normal urinary tract. *Proc Natl Acad Sci U S A* **91:**11889–11893. http://dx.doi.org/10.1073/pnas.91.25.11889.

38. Larsson A, Ohlsson J, Dodson KW, Hultgren SJ, Nilsson U, Kihlberg J. 2003. Quantitative studies of the binding of the class II PapG adhesin from uropathogenic *Escherichia coli* to oligosaccharides. *Bioorg Med Chem* **11:**2255–2261. http://dx.doi.org/10.1016/S0968-0896(03)00114-7.

39. Hannan TJ, Totsika M, Mansfield KJ, Moore KH, Schembri MA, Hultgren SJ. 2012. Host-pathogen checkpoints and population bottlenecks in persistent and intracellular uropathogenic *Escherichia coli* bladder infection. *FEMS Microbiol Rev* **36:**616–648. http://dx.doi.org/10.1111/j.1574-6976.2012.00339.x.

40. Schaeffer AJ, Schwan WR, Hultgren SJ, Duncan JL. 1987. Relationship of type 1 pilus expression in *Escherichia coli* to ascending urinary tract infections in mice. *Infect Immun* **55:**373–380.

41. Hung CS, Bouckaert J, Hung D, Pinkner J, Widberg C, DeFusco A, Auguste CG, Strouse R, Langermann S, Waksman G, Hultgren SJ. 2002. Structural basis of tropism of *Escherichia coli* to the bladder during urinary tract infection. *Mol Microbiol* **44:**903–915. http://dx.doi.org/10.1046/j.1365-2958.2002.02915.x.

42. Le Trong I, Aprikian P, Kidd BA, Forero-Shelton M, Tchesnokova V, Rajagopal P, Rodriguez V, Interlandi G, Klevit R, Vogel V, Stenkamp RE, Sokurenko EV, Thomas WE. 2010. Structural basis for mechanical force regulation of the adhesin FimH via finger trap-like beta sheet twisting. *Cell* **141:**645–655. http://dx.doi.org/10.1016/j.cell.2010.03.038.

43. Sauer MM, Jakob RP, Eras J, Baday S, Eriş D, Navarra G, Bernèche S, Ernst B, Maier T, Glockshuber R. 2016. Catch-bond mechanism of the bacterial adhesin FimH. *Nat Commun* **7:**10738. http://dx.doi.org/10.1038/ncomms10738.

44. Thomas WE, Trintchina E, Forero M, Vogel V, Sokurenko EV. 2002. Bacterial adhesion to target cells enhanced by shear force. *Cell* **109:**913–923. http://dx.doi.org/10.1016/S0092-8674(02)00796-1.

45. Thomas WE, Nilsson LM, Forero M, Sokurenko EV, Vogel V. 2004. Shear-dependent 'stick-and-roll' adhesion of type 1 fimbriated *Escherichia coli*. *Mol Microbiol* **53:**1545–1557. http://dx.doi.org/10.1111/j.1365-2958.2004.04226.x.

46. Yakovenko O, Sharma S, Forero M, Tchesnokova V, Aprikian P, Kidd B, Mach A, Vogel V, Sokurenko E, Thomas WE. 2008. FimH forms catch bonds that are enhanced by mechanical force due to allosteric regulation. *J Biol Chem* **283:**11596–11605. http://dx.doi.org/10.1074/jbc.M707815200.

47. Sokurenko EV, Vogel V, Thomas WE. 2008. Catch-bond mechanism of force-enhanced adhesion: counterintuitive, elusive, but ... widespread? *Cell Host Microbe* **4:**314–323. http://dx.doi.org/10.1016/j.chom.2008.09.005.

48. Bouckaert J, Berglund J, Schembri M, De Genst E, Cools L, Wuhrer M, Hung C-S, Pinkner J, Slättegård R, Zavialov A, Choudhury D, Langermann S, Hultgren SJ, Wyns L, Klemm P, Oscarson S, Knight SD, De Greve H. 2005. Receptor binding studies disclose a novel class of high-affinity inhibitors of the *Escherichia coli* FimH adhesin. *Mol Microbiol* **55:**441–455. http://dx.doi.org/10.1111/j.1365-2958.2004.04415.x.

49. Wellens A, Garofalo C, Nguyen H, Van Gerven N, Slättegård R, Hernalsteens J-P, Wyns L, Oscarson S, De Greve H, Hultgren S, Bouckaert J. 2008. Intervening with urinary tract infections using anti-adhesives based on the crystal structure of the FimH-oligomannose-3 complex. *PLoS One* **3:**e2040. http://dx.doi.org/10.1371/journal.pone.0002040.

50. Han Z, Pinkner JS, Ford B, Obermann R, Nolan W, Wildman SA, Hobbs D, Ellenberger T, Cusumano CK, Hultgren SJ, Janetka JW. 2010. Structure-based drug design and optimization of mannoside bacterial FimH antagonists. *J Med Chem* **53:**4779–4792. http://dx.doi.org/10.1021/jm100438s.

51. Wellens A, Lahmann M, Touaibia M, Vaucher J, Oscarson S, Roy R, Remaut H, Bouckaert J. 2012. The tyrosine gate as a potential entropic lever in the receptor-binding site of the bacterial adhesin FimH. *Biochemistry* **51:**4790–4799. http://dx.doi.org/10.1021/bi300251r.

52. Brument S, Sivignon A, Dumych TI, Moreau N, Roos G, Guérardel Y, Chalopin T, Deniaud D, Bilyy RO, Darfeuille-Michaud A, Bouckaert J, Gouin SG. 2013. Thiazolylaminomannosides as potent antiadhesives of type 1 piliated *Escherichia coli* isolated from Crohn's disease patients. *J Med Chem* **56:**5395–5406. http://dx.doi.org/10.1021/jm400723n.

53. Vanwetswinkel S, Volkov AN, Sterckx YGJ, Garcia-Pino A, Buts L, Vranken WF, Bouckaert J, Roy R, Wyns L, van Nuland NAJ. 2014. Study of the structural and dynamic effects in the FimH adhesin upon α-d-heptyl mannose binding. *J Med Chem* **57:**1416–1427. http://dx.doi.org/10.1021/jm401666c.

54. Kalas V, Pinkner JS, Hannan TJ, Hibbing ME, Dodson KW, Holehouse AS, Zhang H, Tolia NH, Gross ML, Pappu RV, Janetka J, Hultgren SJ. 2017. Evolutionary fine-tuning of conformational ensembles in FimH during host-pathogen interactions. *Sci Adv* **3:**e1601944. http://dx.doi.org/10.1126/sciadv.1601944.

55. Chen SL, Hung CS, Pinkner JS, Walker JN, Cusumano CK, Li Z, Bouckaert J, Gordon JI, Hultgren SJ. 2009. Positive selection identifies an in vivo role for FimH during urinary tract infection in addition to mannose binding. *Proc Natl Acad Sci U S A* **106:**22439–22444. http://dx.doi.org/10.1073/pnas.0902179106.

56. Geibel S, Procko E, Hultgren SJ, Baker D, Waksman G. 2013. Structural and energetic basis of folded-protein transport by the FimD usher. *Nature* **496:**243–246. http://dx.doi.org/10.1038/nature12007.

57. Fiege B, Rabbani S, Preston RC, Jakob RP, Zihlmann P, Schwardt O, Jiang X, Maier T, Ernst B. 2015. The tyrosine gate of the bacterial lectin FimH: a conformational analysis by NMR spectroscopy and X-ray crystallography. *Chembiochem* **16:**1235–1246. http://dx.doi.org/10.1002/cbic.201402714.

58. Wright KJ, Seed PC, Hultgren SJ. 2005. Uropathogenic *Escherichia coli* flagella aid in efficient urinary tract colonization. *Infect Immun* **73:**7657–7668. http://dx.doi.org/10.1128/IAI.73.11.7657-7668.2005.

59. Lane MC, Lockatell V, Monterosso G, Lamphier D, Weinert J, Hebel JR, Johnson DE, Mobley HLT. 2005. Role of motility in the colonization of uropathogenic *Escherichia coli* in the urinary tract. *Infect Immun* **73:**7644–7656. http://dx.doi.org/10.1128/IAI.73.11.7644-7656.2005.

60. Pak J, Pu Y, Zhang ZT, Hasty DL, Wu XR. 2001. Tamm-Horsfall protein binds to type 1 fimbriated *Escherichia coli* and prevents *E. coli* from binding to uroplakin Ia and Ib receptors. *J Biol Chem* **276:**9924–9930. http://dx.doi.org/10.1074/jbc.M008610200.

61. Bullitt E, Makowski L. 1995. Structural polymorphism of bacterial adhesion pili. *Nature* **373:**164–167. http://dx.doi.org/10.1038/373164a0.

62. Hahn E, Wild P, Hermanns U, Sebbel P, Glockshuber R, Häner M, Taschner N, Burkhard P, Aebi U, Müller SA. 2002. Exploring the 3D molecular architecture of *Escherichia coli* type 1 pili. *J Mol Biol* **323:**845–857. http://dx.doi.org/10.1016/S0022-2836(02)01005-7.

63. Mu X-Q, Bullitt E. 2006. Structure and assembly of P-pili: a protruding hinge region used for assembly of a bacterial adhesion filament. *Proc Natl Acad Sci U S A* **103:**9861–9866. http://dx.doi.org/10.1073/pnas.0509620103.

64. Miller E, Garcia T, Hultgren S, Oberhauser AF. 2006. The mechanical properties of *E. coli* type 1 pili measured by atomic force microscopy techniques. *Biophys J* **91:**3848–3856. http://dx.doi.org/10.1529/biophysj.106.088989.

65. Zakrisson J, Wiklund K, Axner O, Andersson M. 2012. Helix-like biopolymers can act as dampers of force for bacteria in flows. *Eur Biophys J* **41:**551–560. http://dx.doi.org/10.1007/s00249-012-0814-8.

66. Forero M, Yakovenko O, Sokurenko EV, Thomas WE, Vogel V. 2006. Uncoiling mechanics of *Escherichia coli* type I fimbriae are optimized for catch bonds. *PLoS Biol* **4:**e298–e299. http://dx.doi.org/10.1371/journal.pbio.0040298.

67. Zakrisson J, Wiklund K, Axner O, Andersson M. 2013. The shaft of the type 1 fimbriae regulates an external force to match the FimH catch bond. *Biophys J* **104:**2137–2148. http://dx.doi.org/10.1016/j.bpj.2013.03.059.

68. Puorger C, Eidam O, Capitani G, Erilov D, Grütter MG, Glockshuber R. 2008. Infinite kinetic stability against dissociation of supramolecular protein complexes through donor strand complementation. *Structure* **16:**631–642. http://dx.doi.org/10.1016/j.str.2008.01.013.

69. Alonso-Caballero A, Schönfelder J, Poly S, Corsetti F, De Sancho D, Artacho E, Perez-Jimenez R. 2018. Mechanical architecture and folding of *E. coli* type 1 pilus domains. *Nat Commun* **9:**2758. http://dx.doi.org/10.1038/s41467-018-05107-6.

70. Jass J, Schedin S, Fällman E, Ohlsson J, Nilsson UJ, Uhlin BE, Axner O. 2004. Physical properties of *Escherichia coli* P pili measured by optical tweezers. *Biophys J* **87:**4271–4283. http://dx.doi.org/10.1529/biophysj.104.044867.

71. Fällman E, Schedin S, Jass J, Uhlin BE, Axner O. 2005. The unfolding of the P pili quaternary structure by stretching is reversible, not plastic. *EMBO Rep* **6:**52–56. http://dx.doi.org/10.1038/sj.embor.7400310.

72. Andersson M, Fällman E, Uhlin BE, Axner O. 2006. A sticky chain model of the elongation and unfolding of *Escherichia coli* P pili under stress. *Biophys J* **90:**1521–1534. http://dx.doi.org/10.1529/biophysj.105.074674.

73. Andersson M, Fällman E, Uhlin BE, Axner O. 2006. Dynamic force spectroscopy of *E. coli* P pili. *Biophys J* **91:**2717–2725. http://dx.doi.org/10.1529/biophysj.106.087429.

74. Andersson M, Fällman E, Uhlin BE, Axner O. 2006. Force measuring optical tweezers system for long time measurements of P pili stability. Proceedings SPIE 6088, Imaging, Manipulation, and Analysis of Biomolecules, Cells, and Tissues IV, 608810 (21 February 2006). http://dx.doi.org/10.1117/12.642266.

75. Lugmaier RA, Schedin S, Kühner F, Benoit M. 2008. Dynamic restacking of *Escherichia coli* P-pili. *Eur Biophys J* **37:**111–120. http://dx.doi.org/10.1007/s00249-007-0183-x.

76. Andersson M, Axner O, Almqvist F, Uhlin BE, Fällman E. 2008. Physical properties of biopolymers assessed by optical tweezers: analysis of folding and refolding of bacterial pili. *Chemphyschem* **9:**221–235. http://dx.doi.org/10.1002/cphc.200700389.

77. Spaulding CN, Schreiber HL IV, Zheng W, Dodson KW, Hazen JE, Conover MS, Wang F, Svenmarker P, Luna-Rico A, Francetic O, Andersson M, Hultgren S, Egelman EH. 2018. Functional role of the type 1 pilus rod structure in mediating host-pathogen interactions. *eLife* **7:**5145. http://dx.doi.org/10.7554/eLife.31662.

78. Habenstein B, Loquet A, Hwang S, Giller K, Vasa SK, Becker S, Habeck M, Lange A. 2015. Hybrid structure of the type 1 pilus of uropathogenic *Escherichia coli*. *Angew Chem Int Ed Engl* **54:**11691–11695. http://dx.doi.org/10.1002/anie.201505065.

79. Crespo MD, Puorger C, Schärer MA, Eidam O, Grütter MG, Capitani G, Glockshuber R. 2012. Quality control of disulfide bond formation in pilus subunits by the chaperone FimC. *Nat Chem Biol* **8:**707–713. http://dx.doi.org/10.1038/nchembio.1019.

80. Eidam O, Dworkowski FSN, Glockshuber R, Grütter MG, Capitani G. 2008. Crystal structure of the ternary FimC-FimF(t)-FimD(N) complex indicates conserved pilus chaperone-subunit complex recognition by the usher FimD. *FEBS Lett* **582:**651–655. http://dx.doi.org/10.1016/j.febslet.2008.01.030.